

Hugely Enhanced Output Power of Direct-Current Triboelectric Nanogenerators by Using Electrostatic Breakdown Effect

Di Liu, Linglin Zhou, Shaoxin Li, Zhihao Zhao, Xing Yin, Zhiying Yi, Chunlei Zhang, Xinyuan Li, Jie Wang,* and Zhong Lin Wang*

Electrostatic breakdown is a common but generally negative physical phenomenon. Here, efficient conversion of mechanical energy to electric power is achieved by enhanced direct-current triboelectric nanogenerator (DC-TENG) based on contact electrification and electrostatic breakdown. By verifying the high temperature can not only improve the triboelectric charge density but also enhance electrostatic breakdown of air dielectric due to thermionic emission of electrons and avalanche breakdown effect. Meanwhile an appropriate low atmosphere pressure is another favorable factor to air breakdown in DC-TENG. As a result, its output power density is improved by three orders of magnitude at 473 K and 300 Pa compared to that at 298 K and standard atmosphere pressure. These findings not only provide a new paradigm to design high-performance TENG, but realize efficiently harvesting mechanical energy and thermal energy in one device by coupling the two kinds of physical effects.

effect is used to develop a new energy-harvesting technology, direct-current triboelectric nanogenerator (DC-TENG).^[6–9] By coupling of triboelectrification effect (or contact electrification) and electrostatic breakdown, DC-TENG shows great potential for efficient mechanical energy harvesting, even considered as a prototype of lightning energy harvesting. Alike with conventional alternative-current triboelectric nanogenerator (AC-TENG) based on triboelectrification effect and electrostatic induction,^[10–20] the DC-TENG has the advantages of lightweight, small size, a wide choice of materials, and high efficiency even at low frequencies.

Different from AC-TENG, the DC-TENG can directly power electronic devices without the auxiliary rectifier circuits and energy storage units.^[7] More importantly, AC-TENG only converts a slight part of electrostatic energy to electrical energy and the other part is dissipated by electrostatic breakdown,^[21,22] but DC-TENG converts the electrostatic energy to electric energy output by electrostatic breakdown, and its energy dissipation resulted from the surface residual charges can be reduced at higher temperature.^[23] Therefore, a higher energy conversion efficiency may theoretically be achieved by DC-TENG at higher temperature. Meanwhile, comparing with other DC generators based on Schottky knot,^[24] silicon p–n junction,^[25] contact barrier between metal and semiconductor,^[26] and tunneling effect in metal-insulator-semiconductor structure,^[27] whose output voltage cannot be higher than the contact barrier voltage (generally less than 1 V), being difficult to power electronics directly, the DC-TENG has another important advantage of its output voltage easy up to hundreds of volts from the static electricity effect.^[7] However, as an energy harvester, how to further improve its output power density, especially output current, still remains the significant interesting of the DC-TENG investigations.


Here, we innovatively couple the thermal energy enhanced air breakdown and contact electrification in DC-TENGs for simultaneous harvesting mechanical and thermal energy at high temperature. We find that the high temperature is beneficial for enhancing the triboelectric charge density in sliding-mode TENG. Then, we find that both a high temperature and an appropriate low atmosphere pressure are beneficial for air breakdown. As a result, the output power density of DC-TENG

1. Introduction

Electrostatic breakdown is one of the most common physical phenomena, such as the natural phenomenon of lightning,^[1] daily electrostatic discharge in drying environment, and electrostatic discharge failure of the widely used electronic components and integrated circuits (IC).^[2,3] In recent decades, great efforts have been focused on the mechanism of electrostatic breakdown and how to avoid the electrostatic breakdown in electronic devices and electronic systems.^[4,5] Recently, this

D. Liu, Dr. L. Zhou, S. Li, Dr. Z. Zhao, X. Yin, Z. Yi, C. Zhang, X. Li, Prof. J. Wang, Prof. Z. L. Wang
Beijing Institute of Nanoenergy and Nanosystems
Chinese Academy of Sciences
Beijing 100083, P. R. China
E-mail: wangjie@binn.cas.cn; zhong.wang@mse.gatech.edu

D. Liu, Dr. L. Zhou, S. Li, X. Yin, C. Zhang, X. Li, Prof. J. Wang, Prof. Z. L. Wang
College of Nanoscience and Technology
University of Chinese Academy of Sciences
Beijing 100049, P. R. China
Prof. Z. L. Wang
School of Materials Science and Engineering
Georgia Institute of Technology
Atlanta, GA 30332, USA

 The ORCID identification number(s) for the author(s) of this article can be found under <https://doi.org/10.1002/admt.202000289>.

DOI: 10.1002/admt.202000289

with sliding mode is improved by three orders of magnitude at 473 K and 300 Pa compared with that at 298 K and standard atmosphere pressure. This work not only provides a new paradigm to enhance the output performance of TENG but also realizes that mechanical and thermal energy are simultaneously and efficiently harvested in DC-TENG through a very simple device by coupling the two kinds of physical effects.

2. Results

2.1. The Basic Principle of Our Designed DC-TENG

Contact electrification is a ubiquitous but complicated phenomenon, and it is also the basic principle of the new energy harvesting technology, TENG. Generally, the charges created by contact electrification in TENG can be used by electrostatic induction or electrostatic breakdown, namely the charges from electrostatic induction plus the charges from electrostatic breakdown is the whole charges created by contact electrification (Figure 1a,i). As for the conventional AC-TENG, the

energy flow chart can be summarized as follows (Figure 1a,ii): mechanical energy is converted to electrostatic energy by contact electrification, and the electrical energy is obtained by electrostatic induction but a part of electrostatic energy will be released by electrostatic breakdown to form the energy dissipation, so the energy output will be much less than the energy input.^[21,22] Considering the conventional views of converting thermal energy to electrical energy are by two approaches: thermal energy is converted to mechanical energy and then to electrical energy by electromagnetic induction; thermal energy is directly converted to electrical energy by thermoelectric effect (Figure 1a,iii), both of them have relatively low conversion efficiency.^[28] More importantly, all of the above energy conversion methods have single energy input source, but our living environment always exists mechanical and thermal energy simultaneously. Generally, the simultaneous harvesting of mechanical and thermal energy relies on the two techniques with different structures^[29] and greatly increases the complexity of the whole system due to the mismatch of different energy harvesting technologies. Therefore, a simple structure that can harvest the two types of energy simultaneously and achieve the physical

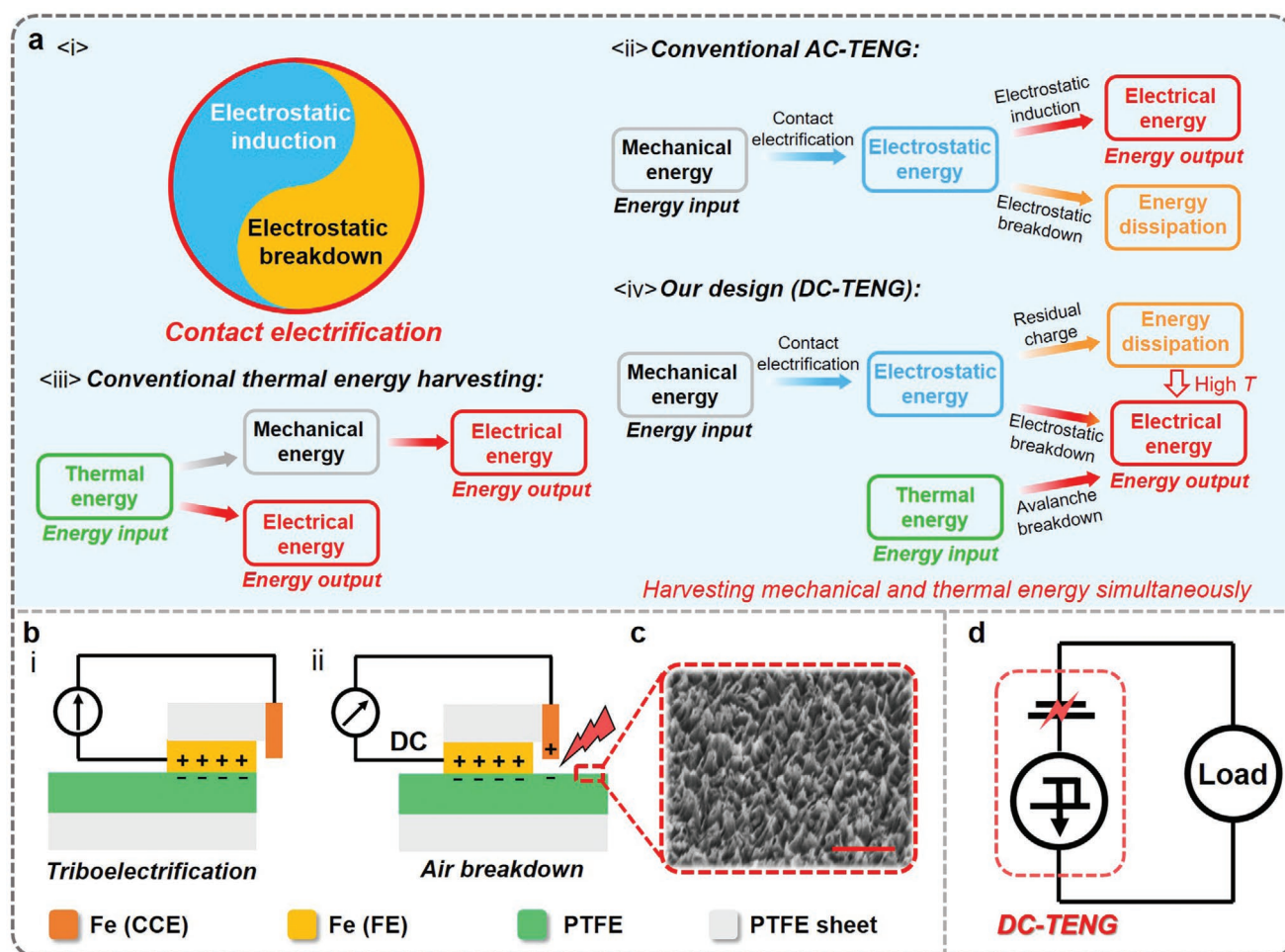


Figure 1. Introduction of electrostatic breakdown for efficient energy harvesting. a) i) The relationship of energy arising from contact electrification, electrostatic induction, and electrostatic breakdown. Energy flow chart of ii) conventional AC-TENG, iii) conventional thermal energy harvesting, and iv) our designed DC-TENG. b) Working mechanism of the sliding mode DC-TENG. c) The scanning electron microscopy (SEM) image of nanowires on the surface of PTFE. Scale bar 1 μm. d) The physics model of the DC-TENG.

coupling of the two effects shows great potential for efficient energy harvesting. The goal of this work is to realize simultaneously harvesting mechanical and thermal energy by using our designed DC-TENG (Figure 1a,iv). First, mechanical energy is converted to electrostatic energy by contact electrification, which is the same as that of conventional AC-TENG; then the electrical energy is obtained by electrostatic breakdown. More importantly, the energy from contact electrification is improved at high temperature and electrostatic breakdown in DC-TENG can be enhanced by avalanche breakdown effect at high temperature. Here the energy dissipation comes from the residual charge on the triboelectric layer, which will be reduced at the higher environmental temperature to further enhance the output electrical energy.^[23]

According to the previous report, sliding mode electrification is more effective to charge the surface than contacting mode and their saturation values of surface charge density are equal.^[11] Therefore, we design a sliding DC-TENG to simultaneously and effectively harvest mechanical and thermal energy. The DC-TENG is mainly composed of three parts: a frictional electrode (FE), a charge collecting electrode (CCE), and a triboelectric layer (Figure 1b; Figure S1, Supporting Information). Its working mechanism is as following: when the FE slides on the triboelectric layer (polytetrafluoroethylene here, PTFE), electrons will transfer from FE to PTFE based on triboelectrification effect (Figure 1b,i). Since the PTFE film is an electret, it can hold a quasi-permanent electric charge. When the slider moves

forward, electrons on the surface of PTFE film will build a high electrostatic field between the PTFE film and CCE. If the electrostatic field exceeds the dielectric strength of the atmosphere between them, the atmosphere will be ionized and become conductive. Electrons will transfer from the surface of PTFE to the CCE (Figure 1b,ii), that is, the CCE is rationally placed to induce air breakdown, creating artificial lightning. Instead of allowing air breakdown to happen spontaneously and having its energy dissipated in a conventional TENG, the CCE effectively collects these charges and energy. To further enhance both contact electrification and air breakdown, we etched the nanostructures on the surface of PTFE film by the inductively coupled plasma (ICP) technique (Figure 1c). The physics model of this DC-TENG is composed of an electric charge source and a unidirectional broken-down capacitor between the CCE and PTFE film (Figure 1d).

2.2. Effects of Atmosphere Pressure and Temperature on Contact Electrification and Air Breakdown

First, we adopt a conventional sliding mode AC-TENG to reveal the effects of atmosphere pressure and temperature on contact electrification and air breakdown in a designed high vacuum system with heater (Figure 2a,b; Figure S2, Supporting Information). As shown in Figure 2c, the output charge density of the sliding mode AC-TENG in high vacuum

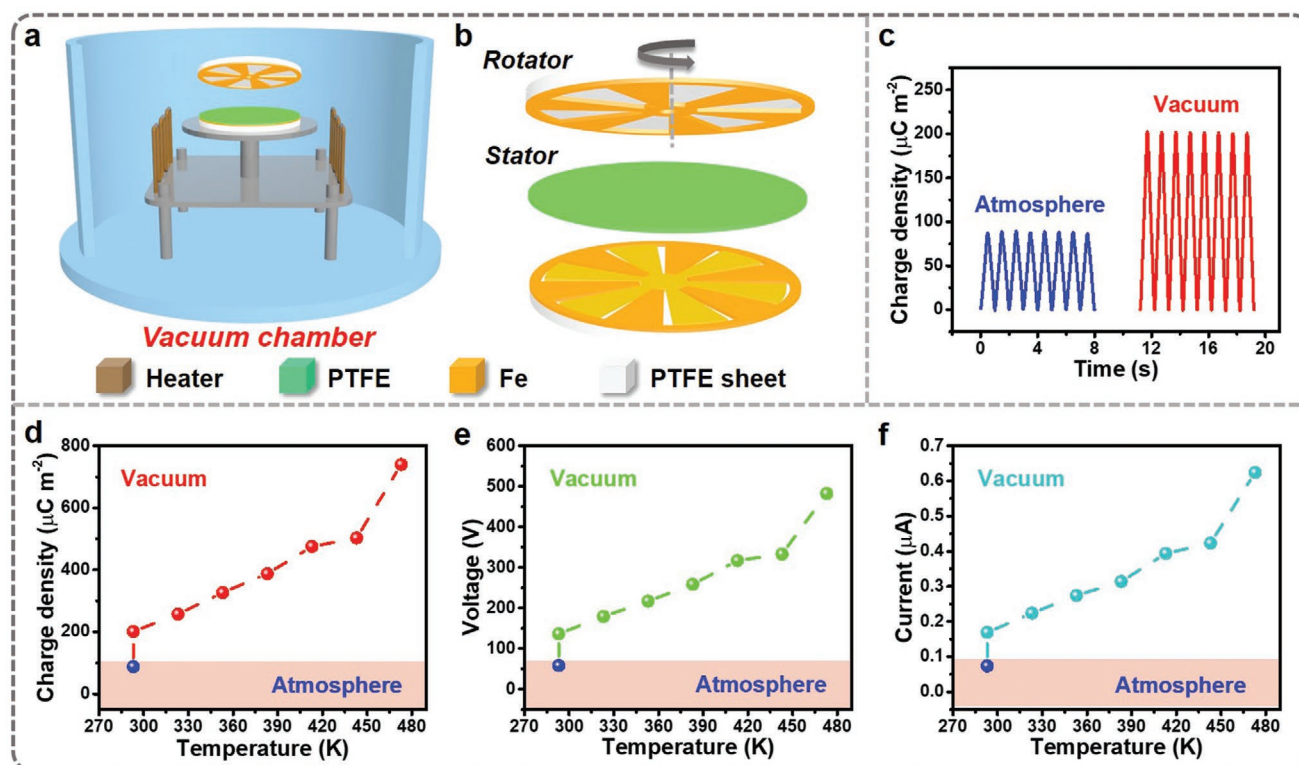


Figure 2. Effects of atmosphere pressure and temperature on contact electrification, air breakdown. a) Schematic illustration of AC-TENG in the measurement platform. b) The schematic diagram of a sliding mode AC-TENG. c) Output charge density of the sliding mode AC-TENG in atmosphere and vacuum environment. d) Output charge density, e) open-circuit voltage, and f) short-circuit current of the sliding mode AC-TENG at various temperatures under standard atmosphere pressure and 5×10^{-5} Pa.

environment (around 10^{-5} Pa) is much higher than the value at atmosphere pressure, which indicates that the output charges of AC-TENG are generally less than contact electrification due to the phenomenon of air breakdown, agreeing well with the previous results.^[21] The corresponding open-circuit voltage and short-circuit current also suggest that as shown in Figure S3, Supporting Information. Therefore, the high vacuum system is used to avoid the air breakdown and eliminate the effects of environmental factors including humidity and gas composition to reveal the effect of temperature on the contact electrification and the output performance of sliding mode TENG (Figures S4–S6 and Note S1, Supporting Information), which may provide a new method for the research on the mechanism of contact electrification and TENGs.

We further investigate the effect of temperature on the output performance of a sliding mode TENG at high vacuum environment (around 5×10^{-5} Pa). We find that the output charge density of the sliding mode TENG increases with the increasing of temperature from 293 to 473 K (Figure 2d). In other words, temperature is beneficial for the contact electrification and output performance of sliding mode TENGs, and even may have a positive impact on sliding mode triboelectrification when air breakdown is avoided. This is also suggested by the output voltage and output current of the sliding mode TENG at various temperatures (Figure 2e,f). Figure S7, Supporting Information, is the detail corresponding output performance. It should be noted that, although the temperature has little effect on contact electrification from the microcosmic perspective,^[23] the triboelectric charge density significantly increases with the temperature here. The reason may be that the higher temperature will increase the contact intimacy between the electrode and triboelectric layer (PTFE, here) from macrocosmic perspective.

2.3. The Coupling of Mechanical and Thermal Energy in DC-TENG

Then, we fabricated a rotary mode DC-TENG to simultaneously harvest mechanical and thermal energy at various atmosphere pressures and temperature in a high vacuum system with heater (Figure 3a,b; Figure S8, Supporting Information). The inset of Figure 3b is the zoomed-in illustration of the stator, where D is the gap distance for air breakdown. The output charge of the DC-TENG first increases then decreases with the decreasing of atmosphere pressure (Figure 3c; Figure S9, Supporting Information). The maximum value is achieved at around 300 Pa where the minimum breakdown voltage of air occurs. The comparison experiment of atmosphere electrostatic breakdown in atmosphere pressure and low pressure also confirm that a relative low pressure is easier for air breakdown (the inset of Figure 3c; Note S2 and Movie S1, Supporting Information). The amount of charges collected by air breakdown is close to zero at 5×10^{-5} Pa, which agrees with that the air breakdown is avoided at 5×10^{-5} Pa, as mentioned above. The corresponding output voltage and current present similar trends (Figure S10, Supporting Information). These results demonstrate that the high vacuum environment can avoid the air breakdown and the

appropriate low atmosphere pressure will enhance electrostatic breakdown again.

Furthermore, we investigate the effect of the temperature on the output of DC-TENG under 300 Pa at various temperatures. The output charges of the DC-TENG gradually increased exponentially with the increase of temperature (Figure 3d). Figure 3e and Figure S11, Supporting Information, are the corresponding output current and output voltage, which indicate approximately constant current output characteristics. The detailed output performance of the DC-TENG at various temperatures with the pressure of 300 Pa are shown in Figures S12,S13 and Note S3, Supporting Information, and the output charge density of $645 \mu\text{C m}^{-2}$ is obtained at 473 K, which is a new record charge density of DC-TENGs. Comparing with the conventional contact-separation mode TENG requiring a very long time to accumulate charges on the surface of the dielectric layer,^[30] a high charge density of DC-TENG can be achieved by only one cycle sliding triboelectrification, which is crucial to study the upper limit of charges transferred during one cycle contact electrification and to understand the mechanism of contact electrification. By applying an external load, the output current keeps nearly stable at 293 and 473 K, and the corresponding output voltage and output power increase linearly, indicating constant current output characteristics again (Figure 3f; Figure S14, Supporting Information). More importantly, the output power density is improved by 500-fold at 473 K compared with it at 293 K, which is attributed to the enhancement of temperature for electrostatic breakdown. Then, we further studied the output performance of the DC-TENG at various temperatures and atmosphere pressures, and the tested results are plotted in Figure S15, Supporting Information. All the results indicate that the high temperature can significantly enhance the output of DC-TENGs.

There are at least three reasons to explain the enhancing effect of temperature on the output performance of DC-TENGs (Figure 3g): 1) The quantity of charges created by sliding mode triboelectrification can be increased by increasing the temperature, that is, the process of triboelectrification is enhanced (The whole red circle in Figure 1a,i is enlarged.). This is demonstrated in high vacuum environment where air breakdown is avoided as mentioned above. 2) The thermionic emission effect will reduce the residual charges on the triboelectric layer to decrease the energy dissipation of DC-TENG. This is verified in microscopic environment using atomic force microscopy and Kelvin probe force microscopy (Figure S16, Supporting Information)^[23] and can also be demonstrated by that the difference between charge density from contact electrification and charge density from electrostatic breakdown at 473 K is much smaller than the value at 293 K (Figure S17, Supporting Information). 3) The mean free path of electrons and collide possibility increase with the increasing of temperature. Hence, electrons will gain more energy under an electrostatic field, so the avalanche breakdown would occur more easily (Figure 3h), and then the output charge and current of DC-TENG significantly increases with the increasing of temperature. It indicates a self-amplifying effect for output current in DC-TENG at high temperature and realizes simultaneous harvesting mechanical and thermal energy by DC-TENG.

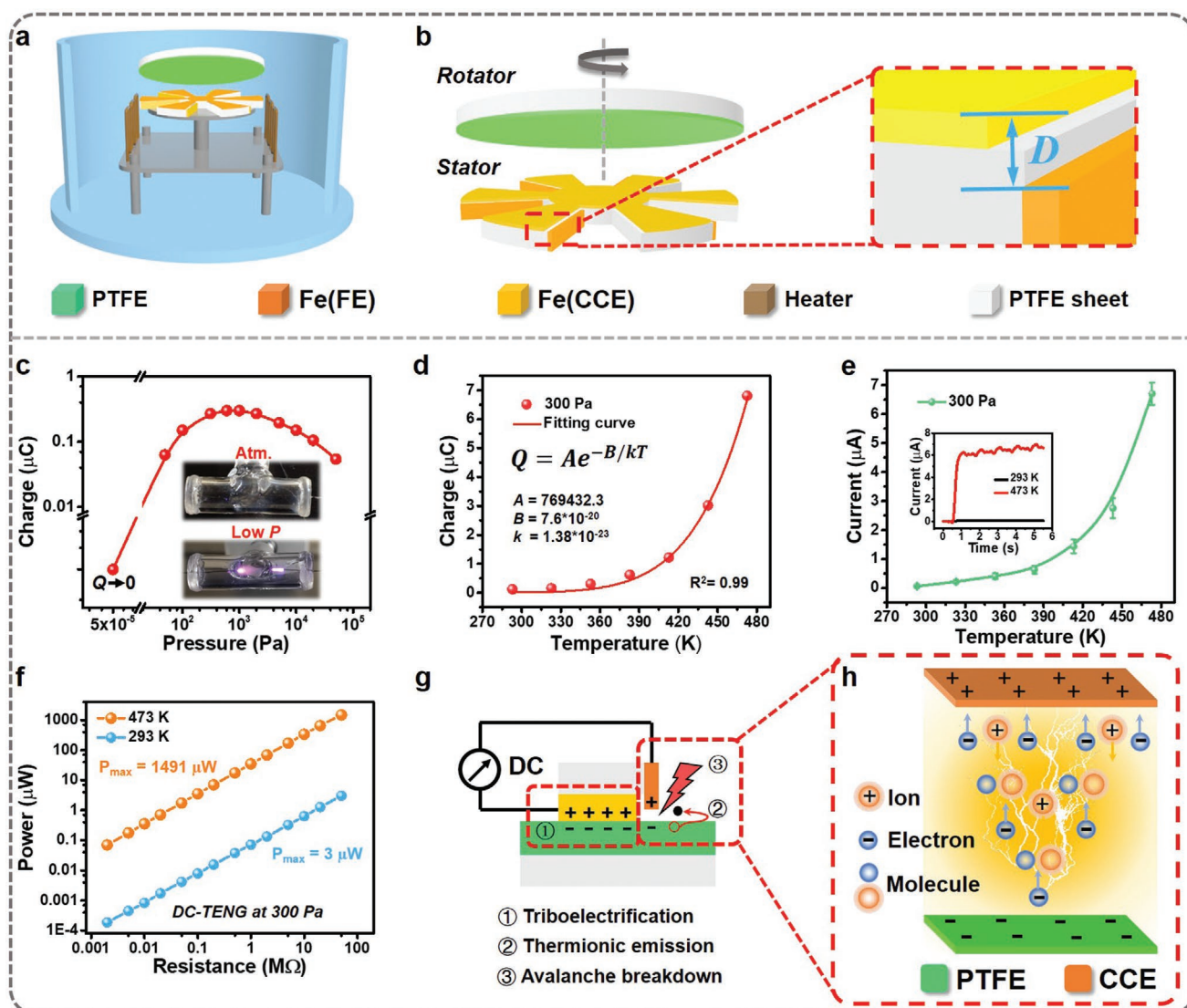


Figure 3. The coupling of mechanical and thermal energy in DC-TENG. a) Schematic illustration of DC-TENG in the measurement platform. b) The schematic diagram of a rotary mode DC-TENG. Inset shows the zoomed-in illustration of its stator. (D represents the gap between CCE and PTFE film.) c) Output charges in per second of a DC-TENG at various atmosphere pressures (Q represents the output charge). d) Transferred charges in per second (fitting data by an exponential function) and e) short-circuit current of a DC-TENG at various temperatures with the pressure of 300 Pa. f) Output power of a DC-TENG with various resistances at 293 and 473 K with the pressure of 300 Pa. g) The physical model of DC-TENGs. h) The avalanche breakdown in DC-TENG.

2.4. Applications of DC-TENG to Directly Drive Electronics

The elevated output performance of DC-TENG in high temperature can be demonstrated by powering various electronics. Figure 4a presents the circuit diagram of the DC-TENG for driving electronics directly without a rectifier or an energy storage unit, which is another advantage of DC-TENG in practical application. Figure 4b shows the voltage curves of three different capacitors charged by a DC-TENG directly, which indicates that the DC-TENG can act as a direct power source for electronics without a rectifier, showing great potential for promoting the miniaturization of self-powered systems. In addition, DC-TENG, as a power source, is able to power electronics and charge capacitors simultaneously, and the corresponding

circuit diagram is shown in Figure S18, Supporting Information. Here, the capacitor is 0.22 mF and the voltage of the capacitor is monitored by a voltmeter. When the capacitor drives the watch alone, the voltage of the capacitor decreases during discharging. If the DC-TENG operates at low temperatures (such as 293 K), the voltage of the capacitor also decreases, indicating that the DC-TENG generates less charges than the watch consumes (Figure 4c). While the DC-TENG operates at high temperatures (such as 473 K), the voltage of the capacitor increases and the watch is powered simultaneously, indicating that the DC-TENG generates more charges than the watch consumes (Figure 4d). For driving a calculator with a higher power consumption, the voltage of the capacitor keeps nearly stable and the calculator is powered simultaneously, showing that the charges generated

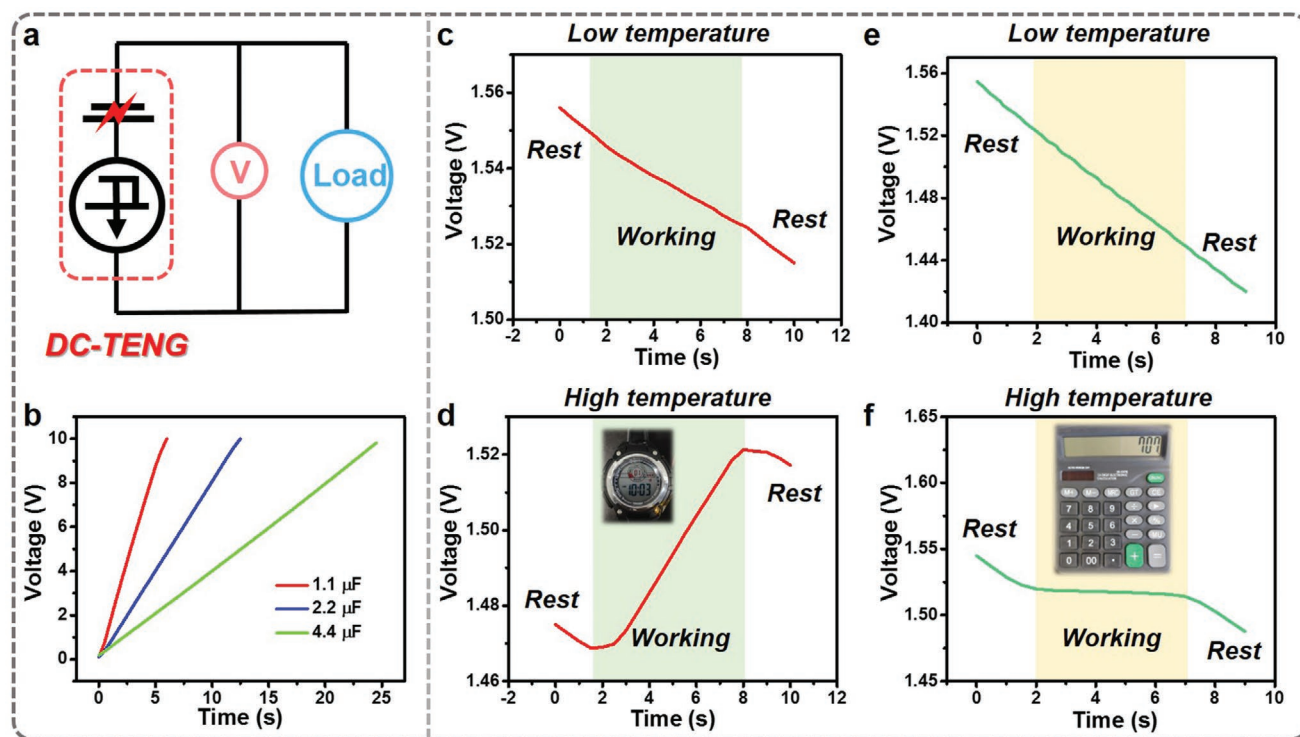


Figure 4. Applications of DC-TENG to directly drive electronics. a) Circuit diagram of the DC-TENG-based self-powered system for driving electronics directly. b) Measured voltage of three different capacitors charged by the DC-TENG directly. Charging curves of a capacitor when the watch is driven by a DC-TENG working in c) low temperature and d) high temperature simultaneously. Charging curves of a capacitor when the calculator is driven by a DC-TENG working in e) low temperature and f) high temperature simultaneously.

by the DC-TENG working at high temperatures are equivalent with the charges consumed by the calculator (Figure 4f). While the DC-TENG working at low temperatures cannot drive the calculator (Figure 4e). Besides adjusting the atmosphere pressure and temperature, the output current of DC-TENG can be further improved by means of structural optimization, parallel method, and increased operation frequency.^[7] In a word, this work provides a novel paradigm for efficient harvesting multiple types of energy simultaneously and a new direction for the optimization of DC-TENG.

3. Conclusion

In this work, we innovatively combine triboelectrification effect and electrostatic breakdown, which is generally considered as a negative effect and is avoided in many fields, realizing simultaneously harvesting mechanical energy and thermal energy in one nanogenerator for the first time. We first reveal the effects of atmosphere pressure and temperature on the triboelectrification effect and air electrostatic breakdown. A high vacuum system with heater was designed to eliminate the effects of other environmental factors and realize accurate measurement, which may provide a new method for the research on the mechanism of contact electrification and TENGs. Without the effects of air breakdown and environmental factors in high vacuum ($\approx 10^{-5}$ Pa), such as humidity and air compositions, the triboelectric charge density of a sliding mode AC-TENG increases

with the increasing of temperature from 293 to 473 K. A record-high triboelectric charge density of $740 \mu\text{C m}^{-2}$ is achieved in a sliding mode TENG by sliding triboelectrification at 473 K, which may be beneficial for understanding the mechanism of triboelectrification and its kinetics.

On the other hand, the moderate low atmosphere pressure can enhance air electrostatic breakdown, therefore, a high charge density of DC-TENG is obtained at around 300 Pa, which is easier to be achieved in practical application, compared with the conventional AC-TENG requiring a high vacuum to reach its maximum output ($\approx 10^{-5}$ Pa). More importantly, the charge density of DC-TENGs increases exponentially with the increasing of temperature due to the enhanced triboelectrification and air breakdown. Therefore, the output power density of the DC-TENG is enhanced by three orders of magnitude at 473 K and 300 Pa compared with that at 298 K and standard atmosphere, which enables it easier to drive wearable electronic devices and the sensors in the internet of things (IoTs) directly.

In a word, the DC-TENG can simultaneously and efficiently harvest mechanical and thermal energy, and have unlimited potential at higher temperatures if high temperature resistant triboelectric materials are developed. Future work will involve developing new triboelectric materials with higher work temperature and adopting more easily broken down air medium to further improve the output performance of DC-TENG. This work can not only provide a new direction for guiding the design of high-performance nanogenerators, but also promote the understanding of the effects of atmosphere pressure

and temperature on contact electrification and electrostatic breakdown.

4. Experimental Section

Preparation of Nanostructures on the Surface of PTFE Film: The nanostructures on the surface of PTFE film was realized by ICP etching system (SENTECH/SI 500). A piece of PTFE film with a thickness of 50 μm was first cleaned by alcohol and deionized water. Then, a thin film of Au (Aurum) as a mask was sputtered onto the surface of PTFE film with 10 s. Finally, this PTFE film was placed into the chamber of the etching system and etched by the ICP. The power of generating plasma and accelerating plasma were 400 and 100 W, respectively. The reaction gases, which induced in the ICP chamber, were Ar, O₂, and CF₄ with flow ratios of 15.0, 10.0, and 30.0 sccm (standard cubic centimeter per minute), respectively.

Fabrication of the AC-TENG: Rotator: i) A round shape of PTFE sheet was cut as the substrate with the diameter of 30 mm and a thickness of 3 mm using a laser cutter (PLS6.75, Universal Laser Systems). ii) A semicircle metal plate was cut as electrode with dimensions of 30 mm (diameter) by 100 μm (thickness) and was pasted on the surface of PTFE sheet. Stator: i) A round shape of PTFE sheet was cut as the substrate with a diameter of 30 mm and a thickness of 3 mm using a laser cutter. ii) Two semicircle metal plates were cut as electrodes with dimensions of 30 mm (diameter) by 100 μm (thickness) and were pasted on the surface of PTFE sheet. iii) The PTFE film was adhered on metal plates as the triboelectric layer with the diameter of 32 mm and a thickness of 50 μm . iv) Both two metal plates were connected by high temperature resistant wires for electrical measurement.

Fabrication of the DC-TENG: Rotator: i) A disc-shaped PTFE sheet was cut as the substrate using a laser cutter. The substrate had a diameter of 80 mm and a thickness of 5 mm. ii) A piece of foam was adhered on the surface of the PTFE sheet with the same size as the buffer. iii) A PTFE film was pasted on the surface of the foam with dimensions of 80 mm (diameter) by 50 μm (thickness). Stator: i) A disc-shaped PTFE sheet was cut as the substrate (diameter, 80 mm; thickness, 5 mm) using a laser cutter. The substrate had a collection of radially arrayed sectors with a central angle of 30°. ii) The metal plate was cut with the same shape of substrate and pasted it on the surface of PTFE sheet, and there was a gap of about 1 mm between the metal plate and the sector edge. The metal plate as the FE. iii) Many rectangle metal plates were cut with the dimensions of 3 cm (length) by 5 mm (width) by 100 μm (thickness) and pasted them at the left sector edge of the substrate along the vertical direction with a small gap between the surface of the PTFE film and the metal plates. All the metal plates were connected as a CCE together. Both metal plates were connected by high temperature resistant wires for electrical measurement.

Electrical Measurement and Characterization: The SEM image of the surface of PTFE was taken with a Hitachi field emission scanning electron microscopy (SU 8020). A programmable electrometer (Keithley Instruments model 6514) was adopted to measure the short-circuit current and transferred charges of TENGs. A designed high vacuum system with heater fabricated with a rotary motor, which could achieve rotating motion and contact separation with a cam, was adopted for building a stable test environment. The vacuum was monitored by a low vacuum ionization gauge and a high vacuum ionization gauge. The temperature was monitored by a vacuum thermocouple gauge. The capacitance and voltage of capacitor were monitored by a potentiostat (Bio-Logic VSP-300, France). NI-6218 was used for data collection. The real-time data acquisition analysis was realized by LabVIEW.

Supporting Information

Supporting Information is available from the Wiley Online Library or from the author.

Acknowledgements

D.L., L.Z., and S.L. contributed equally to this work. Research was supported by the National Key R&D Project from Minister of Science and Technology (2016YFA0202704), National Natural Science Foundation of China (Grant No. 61774016, 5151101243, 51561145021), China Postdoctoral Science Foundation (2019M660587), and Beijing Municipal Science & Technology Commission (Z171100000317001, Z171100002017017, Y3993113DF). Patents have been filed based on the research results presented in this manuscript.

Conflict of Interest

The authors declare no conflict of interest.

Keywords

contact electrification, electrostatic breakdown, mechanical energy harvesting, thermal energy harvesting, triboelectric nanogenerators

Received: March 27, 2020

Revised: April 28, 2020

Published online: June 2, 2020

- [1] V. A. Rakov, M. A. Uman, *Lightning: Physics and Effects*, Cambridge University Press, Cambridge **2003**.
- [2] H. T. Baytekin, B. Baytekin, T. M. Hermans, B. Kowalczyk, B. A. Grzybowski, *Science* **2013**, *341*, 1368.
- [3] S. H. Voldman, *ESD.: Circuits and Devices*, Wiley Press, England **2006**.
- [4] L. Niemeier, L. Pietronero, H. J. Wiesmann, *Phys. Rev. Lett.* **1984**, *52*, 1033.
- [5] B. Chu, X. Zhou, K. Ren, B. Neese, M. Lin, Q. Wang, F. Bauer, Q. M. Zhang, *Science* **2006**, *313*, 334.
- [6] J. Luo, L. Xu, W. Tang, T. Jiang, F. R. Fan, Y. Pang, L. Chen, Y. Zhang, Z. L. Wang, *Adv. Energy Mater.* **2018**, *8*, 1800889.
- [7] D. Liu, X. Yin, H. Guo, L. Zhou, X. Li, C. Zhang, J. Wang, Z. L. Wang, *Sci. Adv.* **2019**, *5*, eaav6437.
- [8] J. Wang, D. Liu, L. Zhou, Z. L. Wang, *Nanogenerators from Electrical Discharge*, IntechOpen Press, China **2019**.
- [9] S. Li, D. Liu, Z. Zhao, L. Zhou, X. Yin, X. Li, Y. Gao, C. Zhang, Q. Zhang, J. Wang, Z. L. Wang, *ACS Nano* **2020**, *14*, 2475.
- [10] F. R. Fan, Z. Q. Tian, Z. L. Wang, *Nano Energy* **2012**, *1*, 328.
- [11] Z. L. Wang, A. C. Wang, *Mater. Today* **2019**, *30*, 34.
- [12] J. Wang, S. Li, F. Yi, Y. Zi, J. Lin, X. Wang, Y. Xu, Z. L. Wang, *Nat. Commun.* **2016**, *7*, 12744.
- [13] Z. Wang, W. Liu, J. Hu, W. He, H. Yang, C. Ling, Y. Xi, X. Wang, A. Liu, C. Hu, *Nano Energy* **2020**, *69*, 104452.
- [14] Y. Liu, W. Liu, Z. Wang, W. He, Q. Tang, Y. Xi, X. Wang, H. Guo, C. Hu, *Nat. Commun.* **2020**, *11*, 1599.
- [15] Y. Zi, C. Wu, W. Ding, X. Wang, Y. Dai, J. Cheng, J. Wang, Z. Wang, Z. L. Wang, *Adv. Funct. Mater.* **2018**, *28*, 1800610.
- [16] C. Wu, H. Tetik, J. Cheng, W. Ding, H. Guo, X. Tao, N. Zhou, Y. Zi, Z. Wu, H. Wu, D. Lin, Z. L. Wang, *Adv. Funct. Mater.* **2019**, *29*, 1901102.
- [17] F. Liu, Y. Liu, Y. Lu, Z. Wang, Y. Shi, L. Ji, J. Cheng, *Nano Energy* **2019**, *56*, 482.
- [18] H. Huo, F. Liu, Y. Luo, Q. Gu, Y. Liu, Z. Wang, R. Chen, L. Ji, Y. Lu, R. Yao, J. Cheng, *Nano Energy* **2020**, *67*, 104150.
- [19] W. Ding, J. Zhou, J. Cheng, Z. Wang, H. Guo, C. Wu, S. Xu, Z. Wu, X. Xie, Z. L. Wang, *Adv. Energy Mater.* **2019**, *9*, 1901320.

- [20] J. Cheng, W. Ding, Y. Zi, Y. Lu, L. Ji, F. Liu, C. Wu, Z. L. Wang, *Nat. Commun.* **2018**, *9*, 3733.
- [21] J. Wang, C. Wu, Y. Dai, Z. Zhao, A. Wang, T. Zhang, Z. L. Wang, *Nat. Commun.* **2017**, *8*, 88.
- [22] X. Xia, J. J. Fu, Y. L. Zi, *Nat. Commun.* **2019**, *10*, 4428.
- [23] S. Lin, L. Xu, C. Xu, X. Chen, A. C. Wang, B. Zhang, P. Lin, Y. Yang, H. Zhao, Z. L. Wang, *Adv. Mater.* **2019**, *31*, 1808197.
- [24] J. Liu, A. Goswami, K. Jiang, F. Khan, S. Kim, R. McGee, Z. Li, Z. Hu, J. Lee, T. Thundat, *Nat. Nanotechnol.* **2018**, *13*, 112.
- [25] R. Xu, Q. Zhang, J. Y. Wang, D. Liu, J. Wang, Z. L. Wang, *Nano Energy* **2019**, *66*, 104185.
- [26] S. S. Lin, Y. H. Lu, S. R. Feng, Z. Z. Hao, Y. F. Yan, *Adv. Mater.* **2019**, *31*, 1804398.
- [27] J. Liu, M. Miao, K. Jiang, F. Khan, A. Goswami, R. McGee, Z. Li, L. Nguyen, Z. Hu, J. Lee, K. Cadien, T. Thundat, *Nano Energy* **2018**, *48*, 320.
- [28] K. Nan, S. D. Kang, K. Li, K. J. Yu, F. Zhu, J. Wang, A. C. Dunn, C. Zhou, Z. Xie, M. T. Agne, H. Wang, H. Luan, Y. Zhang, Y. Huang, G. J. Snyder, J. A. Rogers, *Sci. Adv.* **2018**, *4*, eaau5849.
- [29] S. Wang, Z. L. Wang, Y. Yang, *Adv. Mater.* **2016**, *28*, 2881.
- [30] C. Zhang, L. Zhou, P. Cheng, X. Yin, D. Liu, X. Li, H. Guo, Z. L. Wang, J. Wang, *Appl. Mater. Today* **2020**, *18*, 100496.